

SLAC-PUB-2169  
IC/HEMP/78/21  
July 1978  
(T/E)

EXPERIMENTAL TEST OF EXCHANGE DEGENERACY  
IN HYPERCHARGE EXCHANGE REACTIONS AT 7 AND 11.5 GeV/c<sup>†</sup>

P. A. Baker, J. S. Chima, P. J. Dornan, D. J. Gibbs, G. Hall,  
D. B. Miller, T. S. Virdee, and A. P. White

Imperial College, London, England

J. Ballam, J. Bouchez,<sup>(a)</sup> J. T. Carroll, C. V. Cautis, G. B. Chadwick,  
V. Chaloupka, R. C. Field, D. R. Freytag, R. A. Lewis,<sup>(b)</sup> M. N. Minard,  
K. C. Moffeit, and R. A. Stevens<sup>(a)</sup>

Stanford Linear Accelerator Center  
Stanford University, Stanford, California 94305 U.S.A.

ABSTRACT

We have studied the two pairs of line-reversed reactions:  $\pi^+ p \rightarrow K^+ \Sigma^+$ ;  $K^- p \rightarrow \pi^- \Sigma^+$  and  $\pi^+ p \rightarrow K^+ Y^*(1385)$ ;  $K^- p \rightarrow \pi^- Y^*(1385)$  at two energies: 7 and 11.5 GeV/c. The experiment was conducted in the SLAC 1 m rapid cycling bubble chamber triggered by electronic detectors and an online algorithm. The cross section excess for the  $K^-$  reactions which has shown exchange degeneracy violations at lower energy is still significant but smaller at 7 GeV/c. At 11.5 GeV/c we find that both the helicity-flip and non-flip dominated processes are consistent with exchange degeneracy predictions. Polarization measurements of the  $\Sigma^+$  and  $Y^*$  at both energies support dominance in the production process of exchange degenerate  $K^*(890)$  vector and  $K^*(1490)$  tensor trajectories.

(Contributed paper to the XIX International Conference on High Energy Physics, Tokyo, Japan, 23-31 August 1978.)

---

<sup>†</sup>Work supported by the U.S. Department of Energy and the U.K. Science Research Council.

(a) Present address: DPhPE, CEN-Saclay, B.P. No. 2, F-91190, Gif-sur-Yvette, France.

(b) Present address: Physics Department, Michigan State University, East Lansing, Michigan 48823, U.S.A.

## 1. INTRODUCTION

We present results on the reactions:



at 7 and 11.5 GeV/c. In addition to the differential cross sections, measurement of the parity violating hyperon decays enables the polarization of the  $\Sigma$  or  $Y^*$  to be measured. The reactions are expected to be dominated by vector and tensor  $K^*$  exchange. If these Regge-trajectories are exchange degenerate, equal cross sections for the line-reversed pairs (1a,b) and (2a,b) are predicted as well as equal and opposite hyperon polarization. If the vector and tensor  $K^*$  also have the same residues (strong exchange degeneracy), the polarizations are predicted to be zero. Lower energy data has shown violations of these predictions as the cross section for the  $K^-$  induced reactions has exceeded that from the  $\pi^+$  reaction by a factor of 2 to 4. The results presented at 11.5 GeV/c are also discussed elsewhere<sup>1</sup> and are included here for comparison.

## 2. EXPERIMENTAL DETAILS

The experiments were performed in the SLAC 40" rapid cycling bubble chamber with the flash triggered by an online signature of a fast outgoing  $K^+$  from the  $\pi^+$  induced reactions (1a) and (2a); for reactions (1b) and (2b) the signature was for a fast outgoing  $\pi^-$ . A description of the

experimental setup and trigger has been given elsewhere.<sup>2</sup> The trigger logic was essentially identical at the two energies and very similar for the  $\pi^+$  and  $K^-$  induced reactions. Biasses from the trigger affected only the fast outgoing particles and, therefore, required only an acceptance correction. Below  $|t - t_{\min}| = 0.02 \text{ (GeV/c)}^2$  a correction was required for beam veto logic in the trigger. In the 7 GeV/c data a correction was required above  $|t - t_{\min}| = 0.4 \text{ (GeV/c)}^2$  due to the geometrical acceptance of the downstream system. At 11.5 GeV/c geometrical corrections are not required below  $|t - t_{\min}|$  of 1  $\text{(GeV/c)}^2$ . The acceptance at 7 GeV/c for reaction (1a) is given in Fig. 1. It is very similar for the other reactions at that energy.

Normalization corrections due to trigger dead times, counter inefficiencies and interactions and decays of the beam and trigger particles are essentially the same in both  $\pi^+$  and  $K^-$  exposures. Corrections peculiar to the  $\pi^+$  exposure result from  $\mu$  contamination in the  $\pi^+$  beam and lost triggers caused by pileup in the large downstream Cerenkov counter used for identification of the outgoing particles. For the  $K^-$  exposure a  $\mu$  veto was included to eliminate triggers from  $K^-$  decays and a correction for  $\pi$  punch through was applied. We estimate an overall systematic uncertainty of 10% in the cross section, but the relative uncertainty between the  $\pi^+$  and  $K^-$  exposures and between the two energies is less than 8%. Standard bubble chamber corrections to allow for  $\Lambda$ 's or  $\Sigma$ 's decaying too close or too far from the primary vertex were also made.

Events corresponding to the  $\Sigma$  production reactions (1a) and (1b) were found by scanning for 2-prong events with a charged decay and identified by a 4-constraint fit simultaneously at the production and decay

vertices. For the  $Y^*(1385)$  reactions, (2a) and (2b), the film was scanned for events with two prongs and a neutral vee ( $\Lambda \rightarrow p\pi^-$ ) which then gave a 7-constraint fit at production and decay vertices. The proportion of  $Y^*(1385)$  decaying to  $\Lambda\pi^+$  was determined by fitting the  $\Lambda\pi^+$  mass spectrum below  $1.55 \text{ GeV}/c^2$  to a Breit-Wigner and incoherent phase space background. For momentum transfers less than  $1 \text{ (GeV}/c)^2$  the background level is  $\leq 10\%$  of the  $Y^*(1385)$  peak (see Fig. 2).

3. THE REACTIONS  $\pi^+p \rightarrow K^+\Sigma^+$  and  $K^-p \rightarrow \pi^-\Sigma^+$

Differential cross sections for these reactions to  $|t| = 1 \text{ (GeV}/c)^2$  are shown in Figs. 3(a) and 3(b). They confirm earlier results in showing a simple exponential behavior for  $|t| < 0.4 \text{ (GeV}/c)^2$ . There is no evidence for a turnover in the forward direction, indicating dominance of the non-flip helicity amplitude at least at low momentum transfer. Fits to the cross section of the form

$$\frac{d\sigma}{dt} = Ae^{bt}$$

have been made in the low  $t$  region and the values of  $A$  and  $b$  are given in Table I. At both energies the  $\pi^+$  induced reaction slopes are steeper than for the  $K^-$  reactions, although the difference is less at the higher momentum. Slopes for both reactions increase with energy while the intercepts decrease. The difference of intercepts, however, show a barely significant energy variation. At  $7 \text{ GeV}/c$   $R = (A_{K^-} - A_{\pi^+}) / (A_{K^-} + A_{\pi^+})$  is  $0.063 \pm 0.067$  whereas it is  $-0.021 \pm 0.059$  at  $11.5 \text{ GeV}/c$ . Exchange degeneracy predicts  $R=0$  and within errors this is satisfied at both energies. The integrated cross sections up to  $|t| = 1 \text{ (GeV}/c)^2$  are also given in Table I. They show a marked difference in energy dependence over this

range with the  $K^-$  beam cross section falling much more rapidly than for the  $\pi^+$  beam. To quantify this behavior the conventional parametrization  $\sigma \propto p_{\text{lab}}^{2n}$  has been used. Using our integrated cross sections at 7 and 11.5 we find  $n = 1.18 \pm 0.20$  for  $\pi^+ p \rightarrow K^+ \Sigma^+$  and  $n = 1.61 \pm 0.20$  for  $K^- p \rightarrow \pi^- \Sigma^+$ .

Part of the energy dependence arises from the difference in  $t_{\text{min}}$  at the two energies. In both cases  $t_{\text{min}}$  approaches zero as the energy increases, but this increases the low  $t$  phase space available for the  $\pi^+$  reaction and decreases it for the  $K^-$ . In an attempt to account for this kinematic effect the exponential fit has been used to correct the measured cross sections by

$$\int_{t_{\text{min}}}^0 A e^{bt} dt .$$

This correction increases the  $\pi^+$  cross sections by 3.8 and 1.4  $\mu\text{b}$  at the two energies and decreases the  $K^-$  ones by 4.1 and 1.3  $\mu\text{b}$ . Using the corrected cross sections the values of  $n$  are  $1.24 \pm 0.20$  and  $1.57 \pm 0.20$  showing the  $K^-$  cross section may have a slightly larger energy dependence than the  $\pi^+$  even after corrections for the different kinematic regions.

The only other group to measure this line reversed pair of reactions at two energies with the same experimental technique is a missing mass experiment of Berglund et al.<sup>4</sup> Their results are not inconsistent with those presented here.

Using our data at both energies for the  $\Sigma$  production reactions and parametrizing the cross sections in the form:

$$\frac{d\sigma}{dt} = f(t) s^{\alpha_{\text{eff}}(t)-2}$$

an effective trajectory may be determined by each of the two reactions. They are shown in Fig. 4. Both are consistent with a trajectory passing through the  $K^*(890)$  and  $K^*(1420)$  poles as expected assuming the reactions are dominated by exchange of the vector and tensor  $K^*$ 's.

The  $\Sigma^+$  polarization results, determined by measurement of the decay asymmetry, are shown in Figs. 3(c) and 3(d). The method of analysis and scanning corrections are discussed in an earlier publication.<sup>5</sup> Our increased statistics confirm the results of our earlier publication showing non-zero  $\Sigma$  polarization for both reactions, but polarizations which, within our experimental precision, are equal in magnitude and opposite in sign. The results show no significant difference at the two energies. This reflection symmetry of the polarization is expected in the weak exchange degeneracy hypothesis.

4. THE REACTIONS  $\pi^+ p \rightarrow K^+ Y^*(1385)$  and  $K^- p \rightarrow \pi^- Y^*(1385)$

The differential cross sections are shown in Figs. 5(a) and 5(b). All have a turnover at low momentum transfer showing dominance of the helicity flip amplitude unlike  $\Sigma$  production. The points have been fitted to the parametrization:

$$\frac{d\sigma}{dt} = (A_1 - A_2(t-t_{\min})) e^{bt}$$

The fit is shown in Fig. 5 and the values of  $A_1$ ,  $A_2$  and  $b$  are given in Table II. The broad features of the energy dependence are very similar to those for  $\Sigma$  production. At 7 GeV/c the value of  $b$  for the  $\pi^+$  reaction is greater than for the  $K^-$  while at 11.5 GeV/c they are the same within errors. The integrated cross sections, also given in Table II, show a substantial difference at 7 GeV/c, but a much smaller one at 11.5 GeV/c. Most of the cross section difference at 11.5 GeV/c results solely from

different kinematics for the two reactions.<sup>1</sup> Parametrizing these cross sections as before,  $\sigma \propto p_{\text{lab}}^{-n}$ , the values of  $n$  obtained are  $1.12 \pm 0.20$  for the  $\pi^+$  reaction and  $1.51 \pm 0.20$  for the  $K^-$  reaction. Corrections for the variation of  $t_{\text{min}}$  are less severe in this case due to the turn-over at low  $t$ ; they are also harder to correct for. However using the parameters from the above fit a correction

$$\int_{-0.01}^{t_{\text{min}}} (A_1 - A_2(t-t_{\text{min}})) e^{bt} dt - \int_{-1.0}^0 (A_1 - A_2 t) e^{bt} dt$$

may be made. This suggests an increase of 1.8 and 1.0  $\mu\text{b}$  to the  $\pi^+$  cross sections at the two energies and a decrease of 2.1 and 0.6  $\mu\text{b}$  to the  $K^-$  cross sections. The corrected cross sections yield  $n$  values of  $1.13 \pm 0.20$  for the  $\pi^+$  reaction and  $1.43 \pm 0.20$  for the  $K^-$  one. The results are very similar to those obtained for the non-flip dominated  $\Sigma$  production.

The polarization of the  $Y^*(1385)$  is obtained by a combined maximum likelihood fit to the  $Y^*$  and  $\Lambda$  decay distributions in terms of the transversity density matrix elements. The method is described in another paper submitted to this conference.<sup>3</sup> The results are shown in Figs. 5(c) and 5(d). In neither reaction is there any significant evidence for non-zero polarization at either energy. While this agrees with strong exchange degeneracy predictions it is also predicted on the basis of the additive quark<sup>6</sup> and Stodolsky-Sakurai<sup>7</sup> models.

## 5. CONCLUSIONS

We have measured the differential cross sections and polarizations for  $\Sigma$  and  $Y^*(1385)$  production in line reversed reactions at 7 and 11.5 GeV/c. The energy dependence is found to depend on the initial state, and not on which hyperon is produced, or whether the production is

non-flip or flip dominated. Our data show a much more severe fall in cross section for the  $K^-$  induced processes with increasing beam momentum than for the  $\pi^+$  ones. As a result, the cross section excess for the  $K^-$  reactions which has shown exchange degeneracy violations at lower energy and is still significant at 7 GeV/c has virtually died away by 11.5 GeV/c. Polarization measurements of the  $\Sigma^+$ , which show reflection symmetry between the  $\pi^+$  and  $K^-$  reactions at both energies, and of the  $Y^*$ , which show zero polarization for both energies, also support dominance in the production process of exchange degenerate  $K^*(890)$  vector and  $K^*(1420)$  tensor trajectories for both the non-flip dominated  $\Sigma$  and flip dominated  $Y^*$  production processes.

#### REFERENCES

1. J. Ballam et al., Stanford Linear Accelerator Center preprint SLAC-PUB-2144 (1978), submitted to this conference.
2. G. B. Bowden et al., Nucl. Instrum. Methods 138, 75 (1976);  
J. Ballam and R. D. Watt, Ann. Rev. Nucl. Sci. 27, 75 (1977);  
R. C. Field, SHF Note 67, Stanford Linear Accelerator Center internal publication, Group BC (1977).
3. J. Ballam et al., "Amplitude Analysis of  $Y^*(1385)$  Production in  $\pi^+ p \rightarrow K^+ Y^*(1385)$  and  $K^- p \rightarrow \pi^- Y^*(1385)$  at 7 and 11.5 GeV/c," submitted to this conference.
4. A. Berglund et al., Phys. Letters 60B, 117 (1975);  
A. Berglund et al., Phys. Letters 73B, 369 (1978).
5. P. A. Baker et al., Phys. Rev. Letters 40, 678 (1978).
6. A. Bialas and K. Zalewski, Nucl. Phys. B6, 449 (1968).
7. L. Stodolsky and J. J. Sakurai, Phys. Rev. Letters 11, 90 (1963).



TABLE I

Integrated Cross Sections and Fit Parameters for  $\pi^+ p \rightarrow K^+ \Sigma^+$  and  $K^- p \rightarrow \pi^- \Sigma^+$ .

Reaction	Momentum GeV/c	A $\mu\text{b}/(\text{GeV}/c)^2$	b $(\text{GeV}/c)^{-2}$	$\sigma_{\text{tot}}^{\#}$ $\mu\text{b}$
$\pi^+ p \rightarrow K^+ \Sigma^+$	7.0	$397 \pm 26$	$9.2 \pm 0.5$	$41.5 \pm 4.7$
	11.5	$246 \pm 12$	$10.5 \pm 0.4$	$23.1 \pm 2.4$
$K^- p \rightarrow \pi^- \Sigma^+$	7.0	$450 \pm 40$	$8.2 \pm 0.7$	$60.0 \pm 7.1$
	11.5	$236 \pm 13$	$9.8 \pm 0.4$	$27.0 \pm 2.9$

\* Cross section integrated from  $t = -1.0$  to  $t_{\text{min}}$ . Includes 10% systematic uncertainty.

TABLE II

Integrated Cross Sections and Fit Parameters for  $\pi^+ p \rightarrow K^+ Y^*(1385)$   
 and  $K^- p \rightarrow \pi^- Y^*(1385)$ .

Reaction	Momentum GeV/c	$A_1$ $\mu\text{b}/(\text{GeV}/c)^2$	$A_2$ $\mu\text{b}/(\text{GeV}/c)^4$	$b$ $(\text{GeV}/c)^{-2}$	$\sigma_{\text{tot}}$ $\mu\text{b}$	*
$\pi^+ p \rightarrow K^+ Y^*(1385)$	7.0	$14 \pm 5$	$596 \pm 104$	$7.1 \pm 0.4$	$12.2 \pm 1.4$	
	11.5	$10 \pm 3$	$326 \pm 25$	$7.0 \pm 0.4$	$7.0 \pm 0.8$	
$K^- p \rightarrow \pi^- Y^*(1385)$	7.0	$25 \pm 6$	$554 \pm 96$	$6.0 \pm 0.4$	$21.4 \pm 2.4$	
	11.5	$13 \pm 3$	$362 \pm 28$	$7.0 \pm 0.4$	$10.1 \pm 1.1$	

\* Cross section integrated from  $t = -1.0$  to  $t_{\text{min}}$ . Includes 10% systematic uncertainty.

FIGURE CAPTIONS

1. Acceptance as a function of  $-t'$  for the reaction  $\pi^+ p \rightarrow K^+ \Sigma^+$  at 7 GeV/c.
2. Invariant mass distribution of the  $\Lambda \pi^+$  system at 11.5 GeV/c. The solid line is the result of the maximum likelihood fit.
3. Differential cross sections and  $\Sigma$  polarizations for the reactions  $\pi^+ p \rightarrow K^+ \Sigma^+$  and  $K^- p \rightarrow \pi^- \Sigma^+$  at 7 and 11.5 GeV/c.
4. Effective trajectories for the  $\pi^+ p \rightarrow K^+ \Sigma^+$  and  $K^- p \rightarrow \pi^- \Sigma^+$  reactions between 7 and 11.5 GeV/c.
5. Differential cross sections and  $Y^*$  polarizations for the reactions  $\pi^+ p \rightarrow K^+ Y^*(1385)$  and  $K^- p \rightarrow \pi^- Y^*(1385)$  at 7 and 11.5 GeV/c.

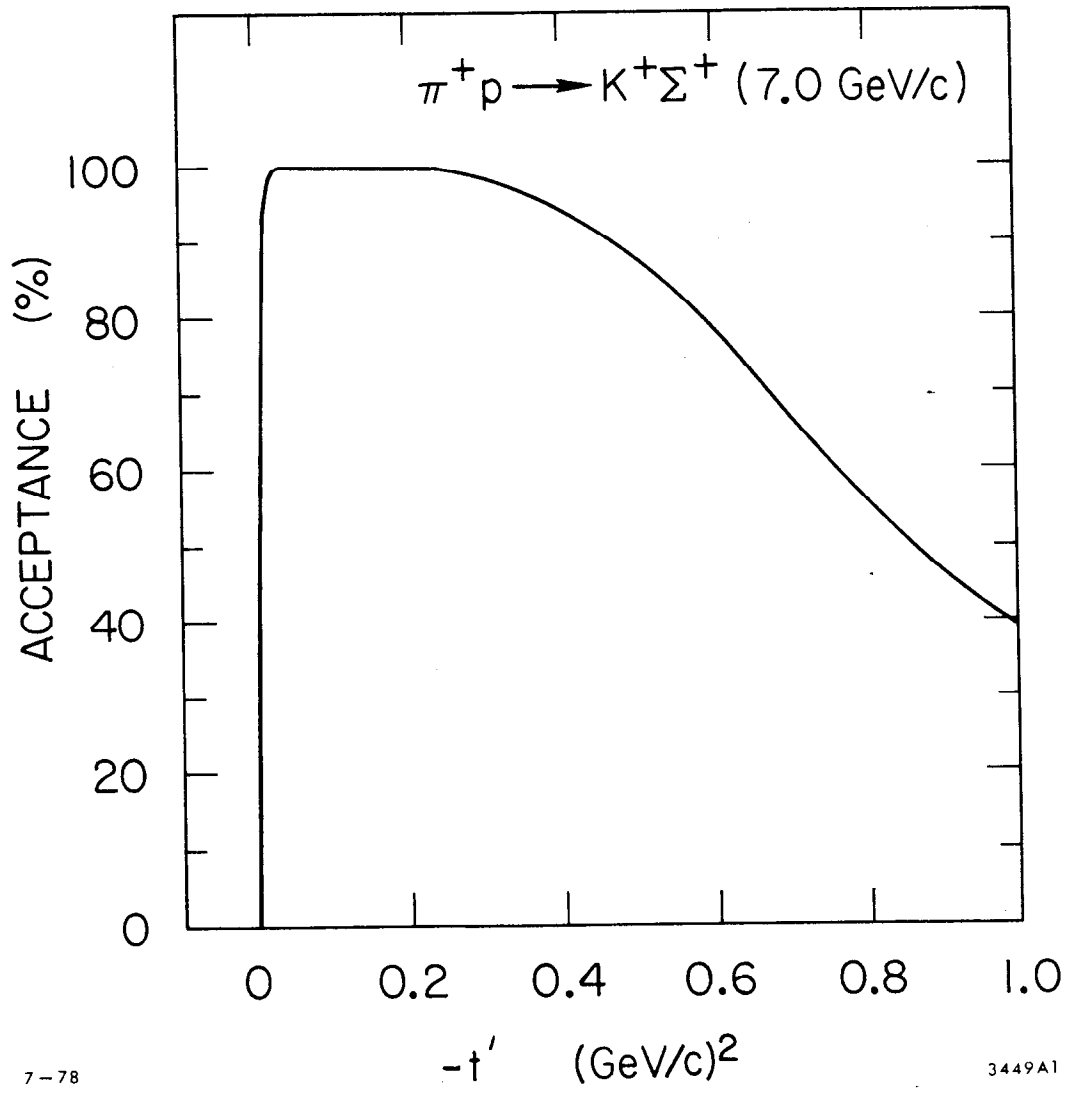


Fig. 1

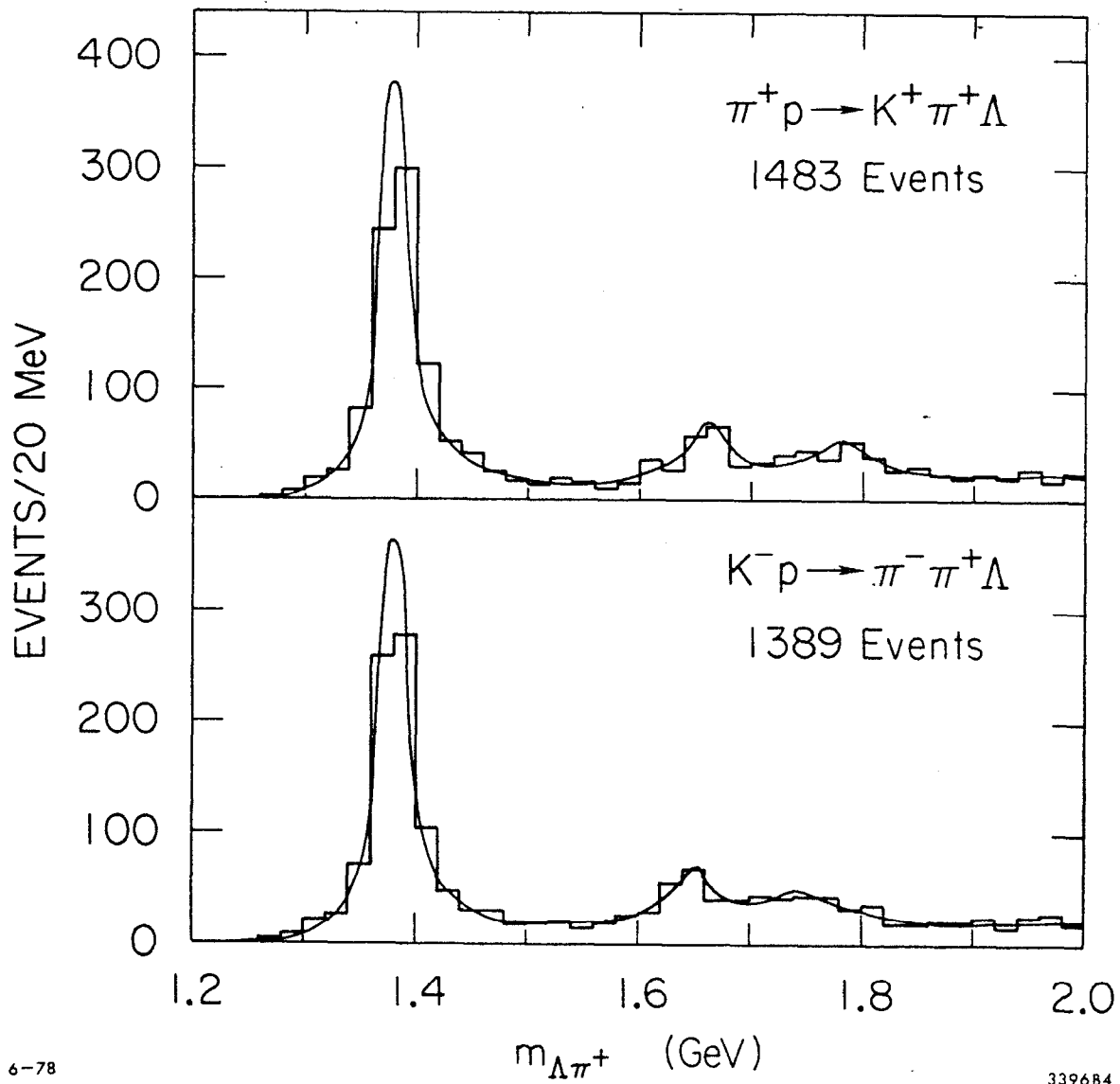


Fig. 2

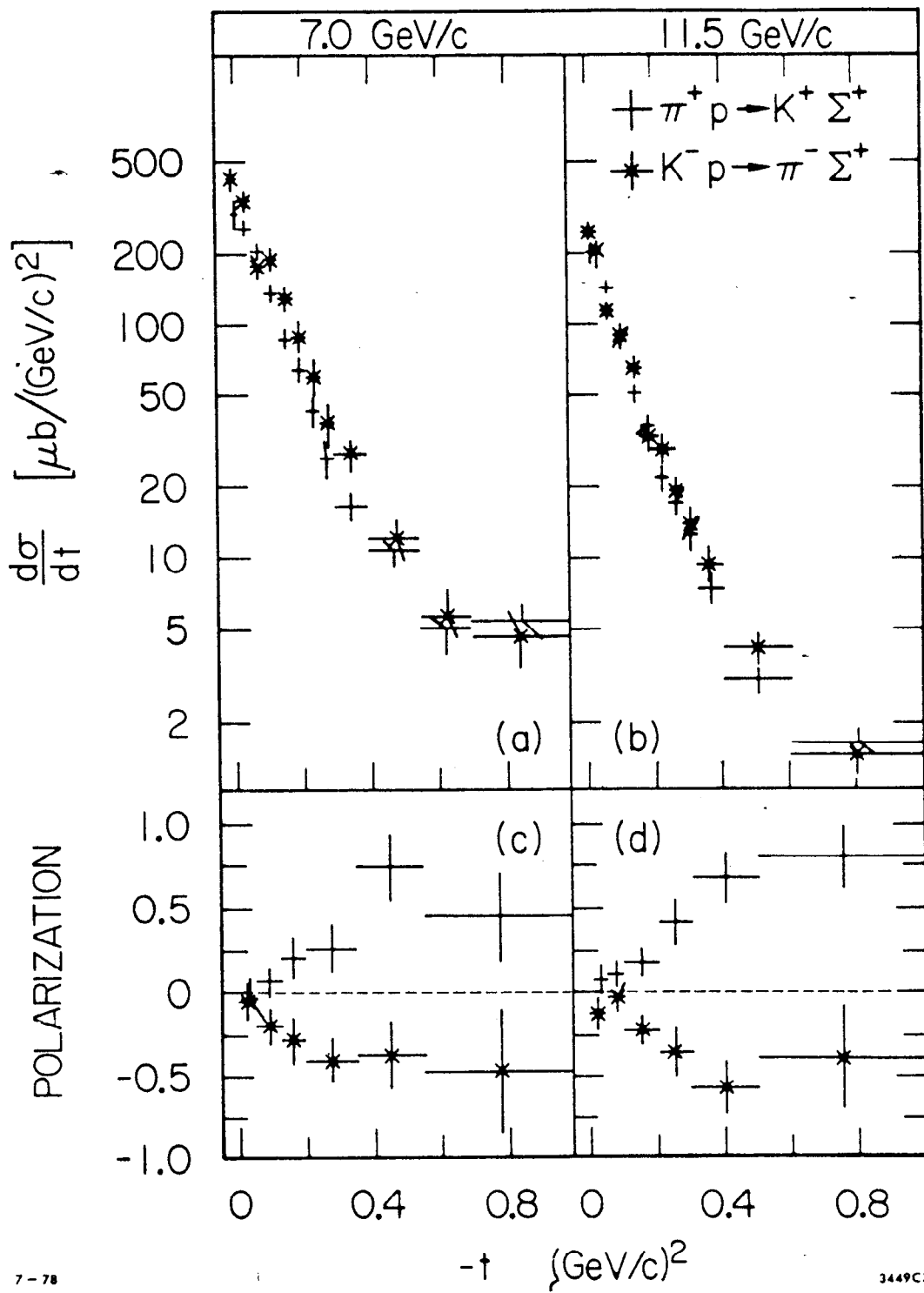


Fig. 3

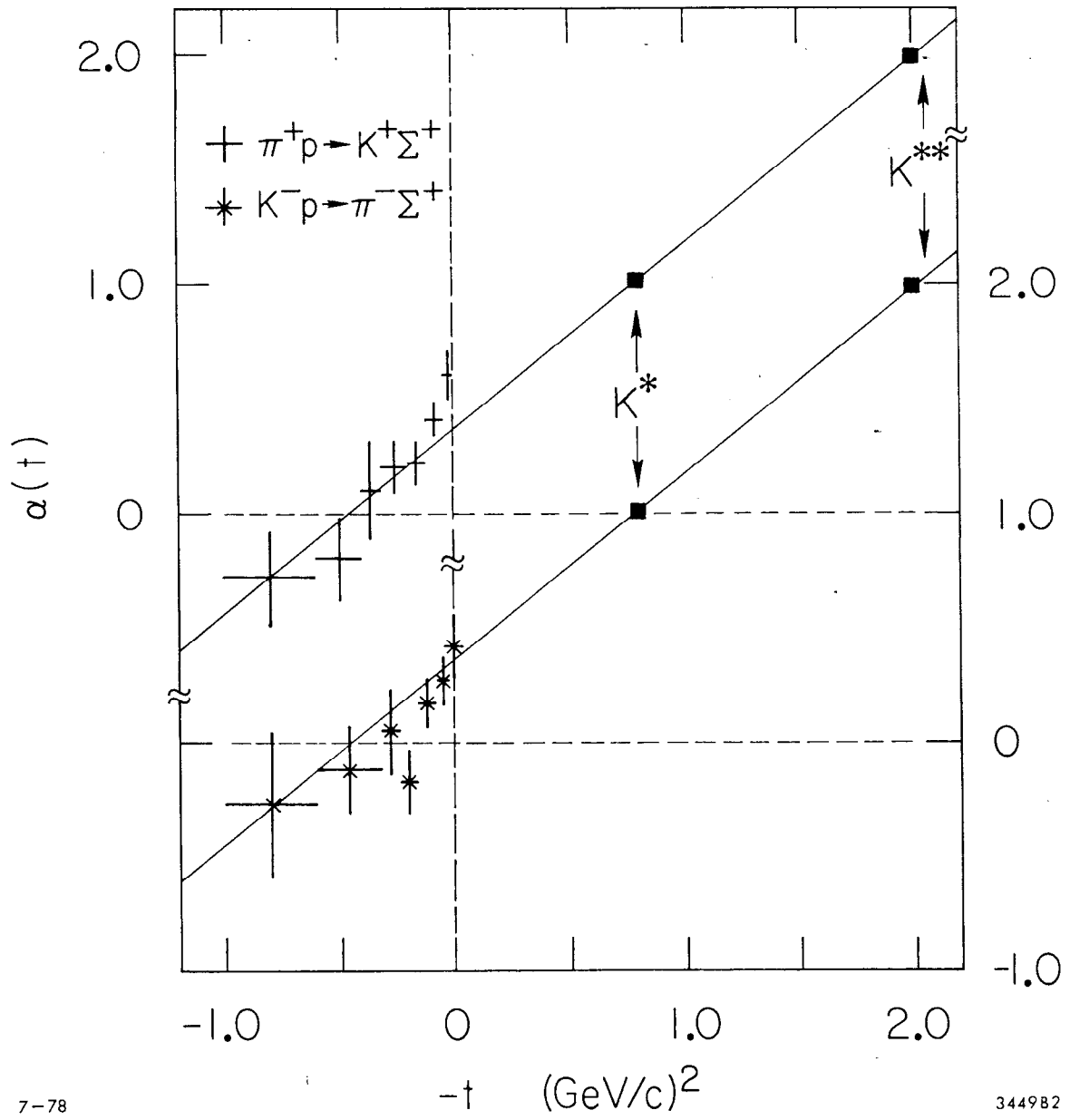


Fig. 4

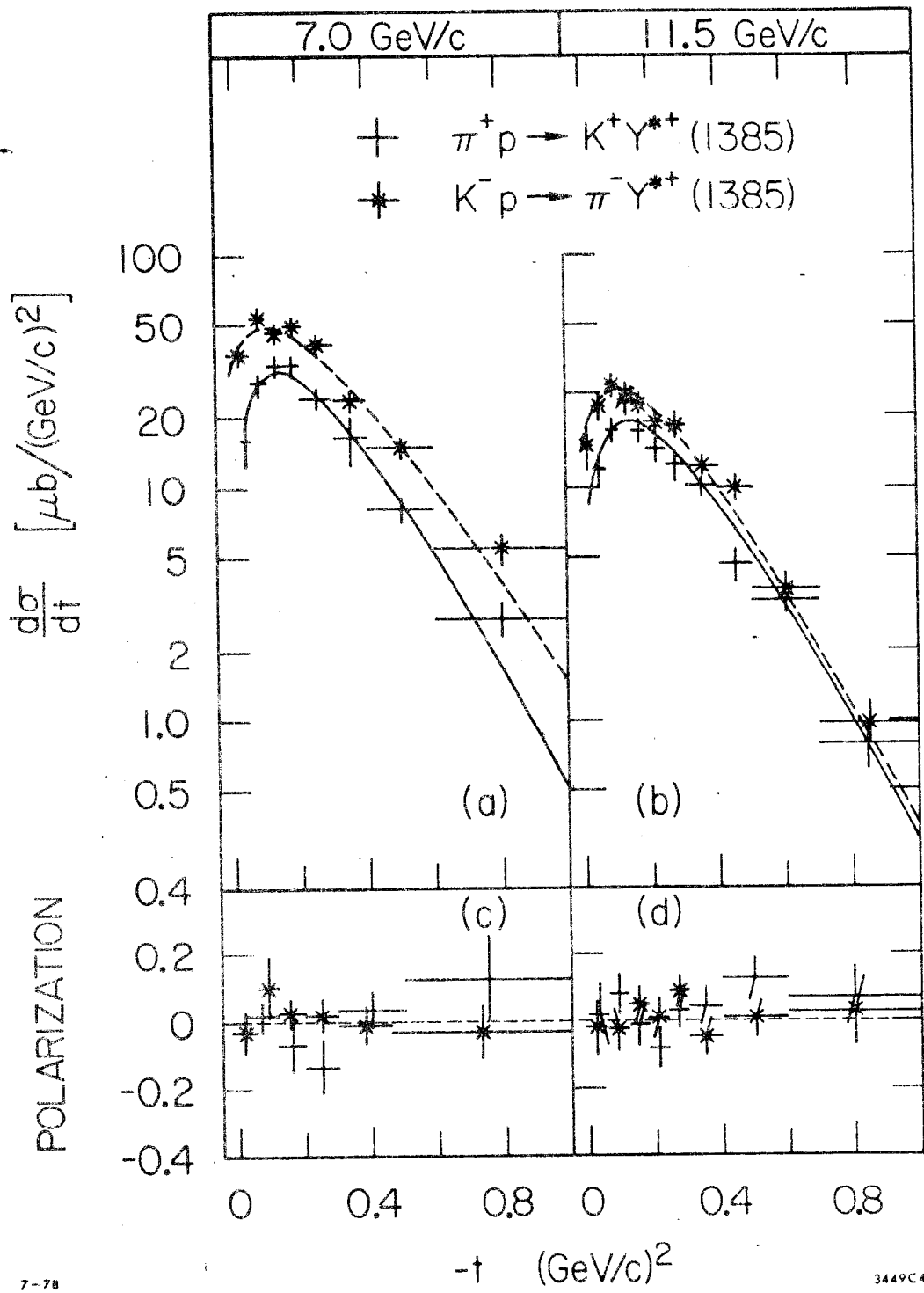


Fig. 5